

<https://doi.org/10.1038/s41514-024-00187-9>

SenMayo transcriptomic senescence panel highlights glial cells in the ageing mouse and human retina

Check for updates

Samyuktha Suresh^{1,7}, Gayathri Karthik ^{1,7}, John F. Ouyang², Vicki Chrysostomou^{1,3}, See Aik Tang¹, Enrico Petretto^{2,4}, Jonathan G. Crowston^{1,3,5} & Katharina C. Bell ^{1,3,6}

There is a growing need to better characterise senescent cells in the CNS and retina. The recently published SenMayo gene panel was developed to identify transcriptomic signatures of senescence across multiple organ systems, but the retina was not included. While other approaches have identified senescent signatures in the retina, these have largely focused on experimental models in young animals. We therefore conducted a detailed single-cell RNA-seq analysis to identify senescent cell populations in the retina of different aged mice and compared these with five comprehensive human and mouse retina and brain transcriptome datasets. Transcriptomic signatures of senescence were most apparent in mouse and human retinal glial cells, with IL4, 13 and 10 and the AP1 pathway being the most prominent markers involved. Similar levels of transcriptional senescence were observed in the retinal glia of young and old mice, whereas the human retina showed significantly increased enrichment scores with advancing age.

Cellular senescence was first described by Hayflick and Moorhead, who observed a gradual decline in replicative potential in cultured human fibroblasts leading ultimately to stable cell cycle arrest. Senescence is a complex, dynamic, and diverse cellular response to various intrinsic and extrinsic stimuli^{1,2}. Cellular senescence is accompanied by alterations in metabolic activity and gene expression profiles as well as the development of a secretory phenotype. This senescence-associated secretory phenotype (SASP) is characterised by the secretion of high levels of pro-inflammatory cytokines, immune modulators, extracellular matrix (ECM) degrading enzymes, growth factors and proteases^{3–5}. Multiple markers need to be evaluated to define senescence. The recently published SenMayo gene set was established in an effort to identify senescent cells in large transcriptomics datasets⁶. This gene panel was derived following extensive literature mining and comprises 125 transcriptomic markers for human and 118 transcriptomic markers for mouse that identified senescent cells in human and mouse datasets⁶.

The observation that senescent cells increase with advancing age in the liver, skin, lung and spleen has led to the assumption that senescence directly contributes to the ageing process^{7,8}. This hypothesis was further fuelled by the discovery that clearance of p16INK4A-positive cells delayed the onset of

age-related diseases in mice⁹. As life expectancy increases, there is an associated increase in the incidence of chronic health conditions associated with ageing¹⁰. Ageing remains a risk factor for many neurodegenerative diseases including Alzheimer's disease¹¹, Parkinson's disease¹² and ocular diseases such as glaucoma and age-related macular degeneration^{13,14} and further work is needed to determine the importance of senescence in this process. In comparison to many other organ systems, our understanding of senescence in the retina and how this changes with physiological ageing remains largely unexplored. There are various factors that complicate the detection of senescence in the retina and CNS. These tissues are comprised of both mitotic and post-mitotic cell populations complicating the identification of senescent cells^{15,16}. In addition, the phenotype of senescent cells itself is largely heterogeneous and dependent on the type of cell, the stressor and the microenvironment¹⁷ making detection of senescence in post-mitotic neurons and glia challenging. Studies have explored the expression of senescence markers mainly in the context of experimental disease of retinal/optic nerve injury models, usually performed in young mice^{18–21}.

In this manuscript, we explored signatures of senescence in the ageing mouse and human retina using the SenMayo panel of senescence markers⁶. Using this gene panel, we find that retinal glial cells were most enriched for

¹Neuroscience and Behavioural Diseases and Eye-ACP, Centre for Vision Research, Duke-NUS Medical School, Singapore, Singapore. ²Programme in Cardiovascular and Metabolic Disorders, Duke-NUS Medical School, Singapore, Singapore. ³Singapore Eye Research Institute, Singapore National Eye Centre, Singapore, Singapore. ⁴Institute for Big Data and Artificial Intelligence in Medicine, School of Science, China Pharmaceutical University, Nanjing, China. ⁵Save Sight Institute, University of Sydney, Sydney, NSW, Australia. ⁶NHMRC Clinical Trial Centre, University of Sydney, Camperdown, NSW, Australia. ⁷These authors contributed equally: Samyuktha Suresh, Gayathri Karthik. e-mail: katharina.bell@sydney.edu.au

the SenMayo panel in both human and mouse retina and show an age-related increase in senescence markers only in the human retina. Interleukin signalling driven by IL-4, -13 and 10 were highly enriched in these cells across species and cell types and the AP1 transcription pathway was additionally observed in SenMayo gene set enriched microglia.

Results

Mouse retinal glial cells are highly enriched for the SenMayo gene panel

Our scRNA mouse retina dataset comprised 63,303 cells from 3-, 12- and 24-month-old retinal samples. Rods, cones, bipolar cells (BCs), amacrine cells (ACs), retinal ganglion cells (RGCs), horizontal cells (HCs), Mueller glia (MG), astrocytes (Asc), microglia (Mic) and Endothelial cells and Pericytes (ECs & Pericytes) were the major cell types identified as clusters in the UMAP (Fig. 1a, Supplementary Fig. 1d–f). A small cluster of retinal blood cells (Ret blood) was also identified. Glial cells and ECs and Pericytes scored the highest in the gene set enrichment analysis (GSEA) (performed at the single-cell level using the escape package) of the SenMayo gene panel (Fig. 1b, c) with ~69% SenMayo-hi astrocytes, ~57% ECs and pericytes, ~47% SenMayo-hi microglial and ~30% SenMayo-hi MG (Fig. 1d). In comparison, retinal neurons had very low numbers of SenMayo-hi cells (ACs- 0.22%, BCs- 0.26%, Cones- 1.2%, HCs- 0%, RGCs- 0.37%, Rods- 0.006%). SenMayo-hi cells were also enriched for two other independently established ageing gene sets – CellAge²² and GenAge²³ and expressed higher levels of *Tgfb2*, a driver of senescence which is not a part of the SenMayo panel^{24,25} (Fig. 1e). Using a third independent senescence gene panel²⁶ (Cherry_2023), we observed again that glial cells had the highest enrichment for senescence-related genes (Supplementary Fig. 2c). Since the microglial cells showed very high SenMayo enrichment score as seen in the density plot (Fig. 1b), we wanted to verify whether this was due to a high proportion of SenMayo genes being microglial marker genes. Using a published retinal microglial gene set (HU_FETAL_RETINA_MICROGLIA)²⁷ as a reference, we removed the 14 overlapping genes from the SenMayo panel. GSEA for this SenMayo-reduced gene set was performed, which resulted in the same enrichment pattern in which we found that retinal glia and ECs & Pericytes had the highest SenMayo (SenMayo-reduced panel) enrichment scores (Supplementary Fig. 2d). To further verify our results, we performed enrichment analysis on another large independent dataset- the mouse retinal atlas from Rui Chen lab (Supplementary Fig. 2g). Here too the SenMayo and the SenMayo-reduced gene panels highlighted glial cells, ECs and Pericytes (Supplementary Fig. 2h, j). Microglial cells scored the highest SenMayo enrichment scores among the cell types (Supplementary Fig. 2i). The various senescence gene panels used here were derived from different experiments and backgrounds and when comparing these different panels, we only detected minimal overlap of the genes, thus strengthening our findings (Supplementary Fig. 8a). We performed cell-cell interaction analysis in our dataset since it is known that senescent cells have a paracrine influence on their neighbouring cells²⁸. Cell-cell interaction analysis of our mouse retina dataset revealed extensive interaction amongst the SenMayo-hi cells themselves and retinal glial and vascular endothelial cells. Interactions were also observed between SenMayo-hi cells with other neuronal cells such as BCs and cones, although to a lesser extent (Fig. 1f, Supplementary Fig. 2e, f). Interaction pathways include neuromodulatory and neuroinflammatory pathways such as pleiotrophin (PTN), prosaposin (PSAP) and neural cell adhesion molecule (NCAM), Midkine (MK) (Fig. 1f). PSAP²⁹, MK³⁰ and PTN³¹ for example are senescence modulating factors and can contribute to SASP factor production.

SenMayo-hi microglia in the mouse retina has the potential to attract immune cells into the retina

Immune cell attraction (“Leukocyte Cell-Cell Adhesion”, “Leukocyte migration”, “Mononuclear cell migration”, “Monocyte Chemotaxis”) and activation (“Macrophage activation”, “T cell activation”) were among the most enriched biological processes (GO-BP) in SenMayo-hi microglial cells (Fig. 2a, b, Supplementary Table 4a), highlighting the role these cells play in immune cell infiltration into the retina.

Among the top upregulated genes in the SenMayo-hi microglia (compared to SenMayo-low microglia), we observed genes from the Jun/Fos transcription factor family such as *Jun* and *Junb*³² as well as other genes related to inflammation and senescence regulation such as *Nfkbia*³³, and *Neat1*³⁴. (Fig. 2c, Supplementary Table 3). Pathway analysis in SenMayo-hi microglia revealed enrichment of interleukin signalling including IL4, 6, 10, 12 and 13, AP1 signalling and Nod-like receptor (NLR) signalling that are all known to modulate senescence and senescence activated secretory phenotype (SASP)^{35–39}. (Fig. 2d, Supplementary Table 4b). *Tgfb1*⁴⁰ and *Ccnd1*(*CyclinD1*)⁴¹ genes, which are downstream of the AP1 pathway, *Il10ra*, *Il10rb*⁴², *Stat1*⁴³, and *Stat3*⁴⁴ which control interleukin signalling, were highly expressed in SenMayo-hi microglia compared the SenMayo-low microglia (Fig. 2e, Supplementary Table 3). To further strengthen our findings, we also analysed the retinal microglia dataset from the Saban lab and found that the SenMayo-hi microglia from these datasets also showed enrichment for IL4/13, IL10, NLR as well as the AP1 signalling pathway (Supplementary Table 12).

SenMayo-hi Mueller glia in the mouse retina are in a highly activated state

GO-BP analysis of SenMayo-hi Mueller glia (Fig. 3a) indicated that they are in an activated state- “Gliogenesis”, “Glial Cell differentiation”, “Astrocyte differentiation” (Mueller glia are very closely related to astrocytes^{45,46}) and have the potential to activate retinal microglia - “Microglial cell activation”. TGF- β signalling and SMAD protein signal transduction, which are involved in SASP factor signalling, were among the enriched pathways²⁴ (Fig. 3b, Supplementary Table 6a). Among the top DEGs, we once again observed several members of the Jun/Fos family, such as *Jun*, *Fos*, *Fosb*, and other senescence modulators such as *Ccn1*⁴⁷ and *Timp3*⁴⁸ (Fig. 3c, Supplementary Table 5). AP1 pathway is similarly enriched in SenMayo-hi Mueller glia (Fig. 3d, Supplementary Table 6b). Other pathways such as the NFAT pathway⁴⁹, IL-4/13 signalling^{36,50,51} and IL6 signalling^{35,36} are also known to play a role in senescence (Fig. 3d, Supplementary Table 6b). Genes such as *Ccnd1*⁴¹, *Cdkn1b*^{52,53} (p27Kip1) which are related to AP1 and *Stat1/3*^{54,55}, *Il18*^{56,57}, and *Anxal1*⁵⁸ (Annexin A1) which are involved in interleukin signalling are more highly expressed in the SenMayo-hi cells compared to the SenMayo-low Mueller glia (Fig. 3e, Supplementary Table 5). Though astrocytes, the other macroglial cell type found in the retina were highly enriched for SenMayo-hi cells, they were detected at low numbers that did not yield itself to statistically significant results.

Human retinal glia is also highly enriched for the SenMayo gene panel

We analysed a published human retina dataset with around 74,000 cells (GEO: GSE148077)⁵⁹ and successfully annotated the various retinal cell types. (Fig. 4a, Supplementary Fig. 3d–f). Similar to the mouse retina dataset, glial cells score high for the SenMayo panel (Fig. 4b). Enrichment scores in the glial cells and endothelial/pericytes were among the highest and the retinal neurons scored much lower (Fig. 4b). Since the microglia scored the highest, scores of this subcluster were used to set the threshold for SenMayo-hi cells (Fig. 4c), which were bimodal like the mouse microglial cells (Supplementary Fig. 4a, b). Microglia (~88%) once again have the highest percentage of SenMayo-hi cells (Fig. 4d). This is followed by endothelial cells (ECs) and pericytes (78%), Asc (54%), MG (17%), ACs (0.62%), RGCs (0.33%), HCs (0.21%), BCs (0.2%), Cones (0.18%), Rods (0.015%) SenMayo-hi cells are enriched for GenAge and CellAge gene sets (Fig. 4e) and also for key senescence-related genes such as MIF and AXL (Fig. 4f). Similar to the mouse gene sets, there was little overlap between the different ageing and senescence gene panels used for the human data (Supplementary Fig. 8b). Like in the mouse dataset, neuroinflammatory and neuromodulatory pathways were key among interactions between SenMayo-hi cells and other retinal cells. Various key cell-cell communication pathways detected in the mouse retina such as PSAP, PTN and NCAM were also identified in the human retina. SPP1 (Osteopontin) was a key interaction partner within the SenMayo-hi cells (Supplementary Fig. 5c).

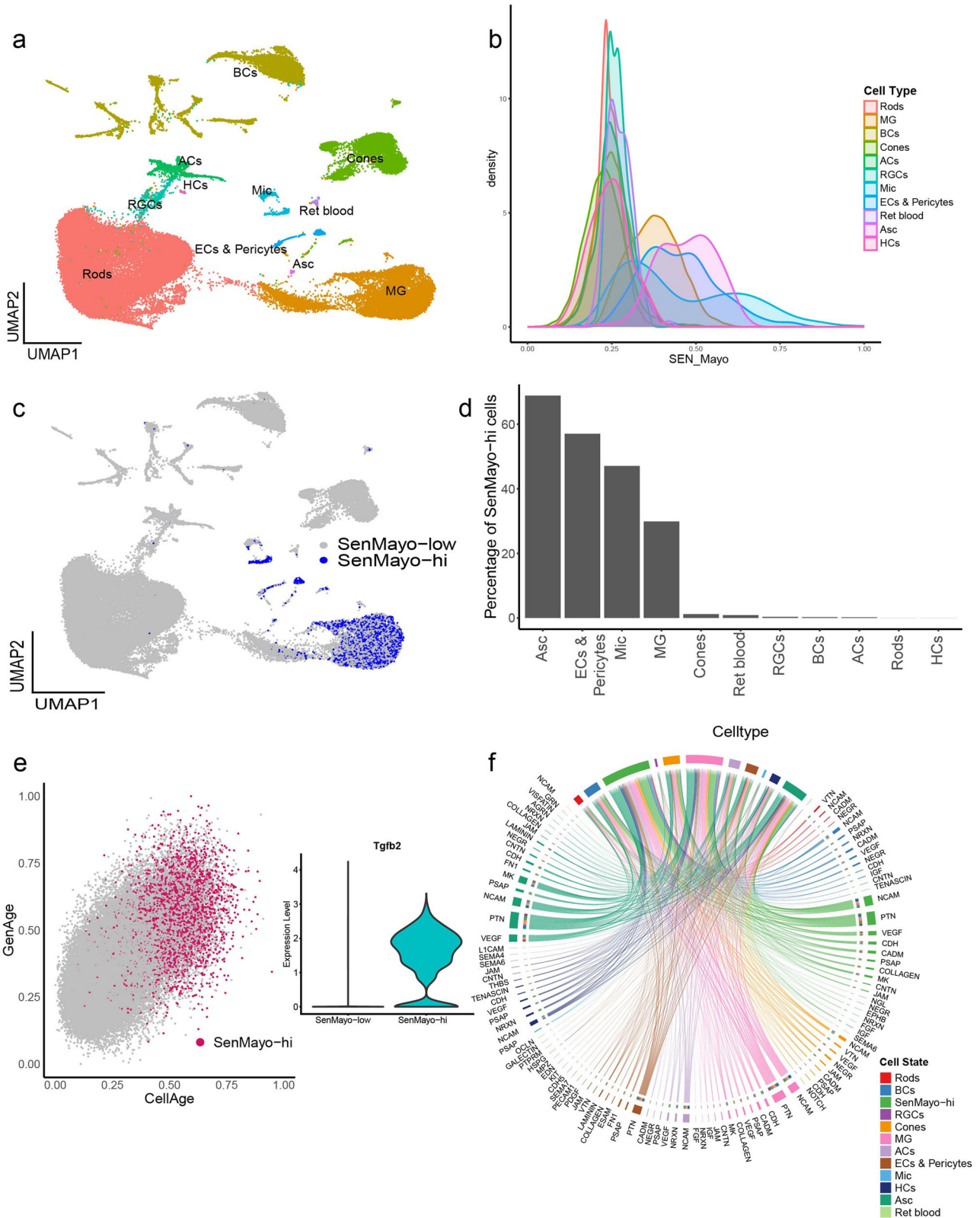


Fig. 1 | “SenMayo-hi” cells detected in the mouse retina mainly correspond with retinal glial cells. **a** UMAP plot of murine retina samples collected from 3-, 12-, and 24-month-old mice representing an ageing series. Cells detected include neurons such as Rods, Cones, Retinal Ganglion Cells (RGCs), Bipolar cells (BCs), Amacrine Cells (ACs), Horizontal cells (HCs), glia including Mueller Glia (MG), Astrocytes (Asc) and Microglia (Mic), Endothelial cell, Pericytes (ECs & Pericytes) and retinal blood cells (Ret blood). **b** Density plot showing the cell type distribution of SenMayo gene panel enrichment scores obtained using the escape package. Mic cells score the

highest. **c** UMAP highlighting the SenMayo-hi cells, which correspond to Mac, Mic, Asc and Endothelial cells. **d** Percentage of SenMayo-hi cells per cell type. **e** SenMayo-hi cells also score high for GenAge and CellAge. Inset: Violin plot shows the upregulation of *Tgfb2* gene expression in SenMayo-hi cells in the mouse retina. **f** Chord diagram representing ligand-receptor (L-R) signalling pathways in the mouse retina, that includes signalling both from and to the SenMayo-hi cells. These cells mainly interact with themselves, suggesting a strong signalling network within this category.

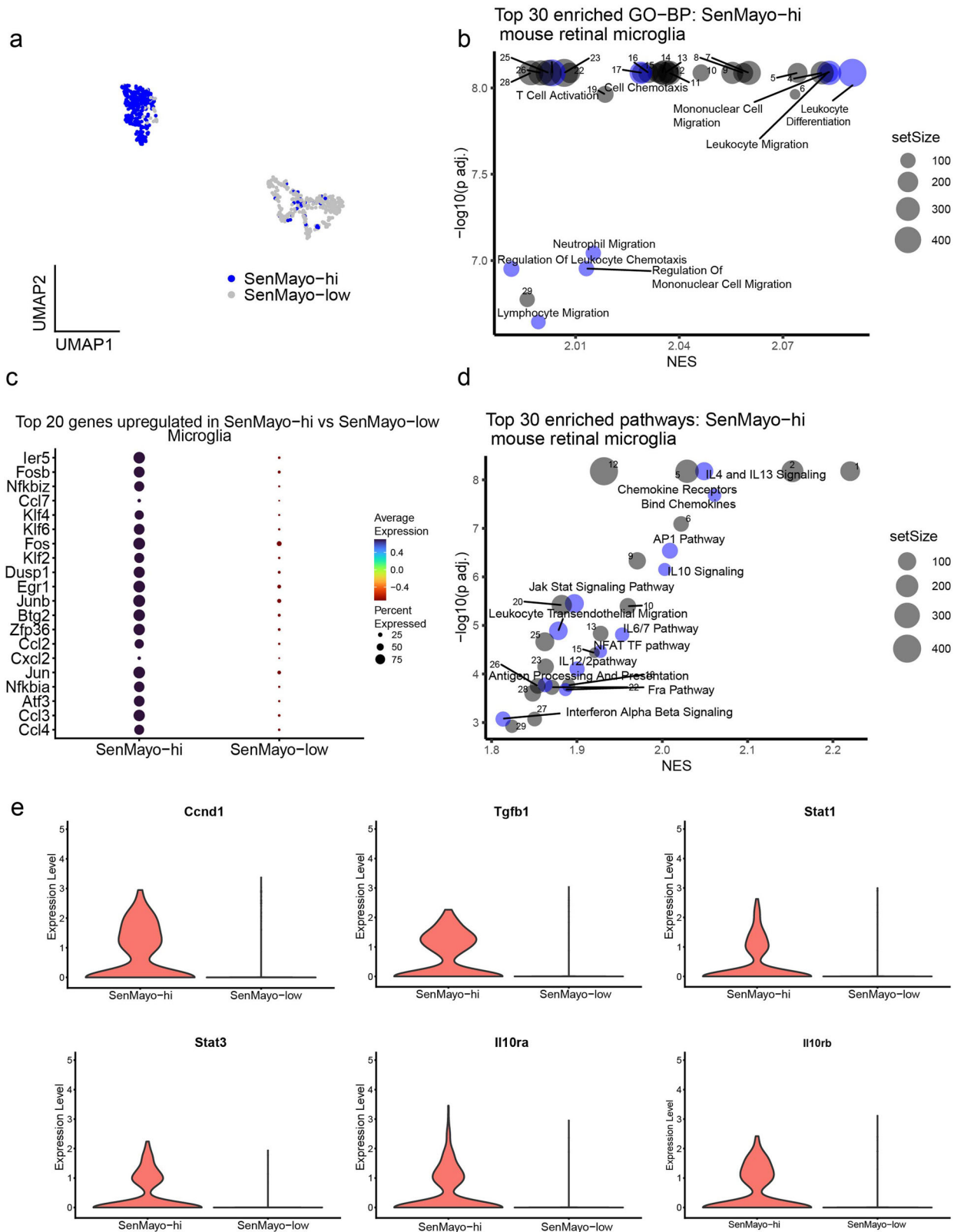


Fig. 2 | SenMayo-hi cells detected in the retinal microglia (Mic). **a** UMAP plot of SenMayo-hi cells in the Mic subcluster. **b** Top 30 enriched biological processes (BP) in SenMayo-hi Mic, with senescence and immune response-related processes highlighted in blue (FDR < 0.01). See the Supplementary Table 4a for a full list. **c** Top 20 genes upregulated in the SenMayo-hi Mic (vs SenMayo-low Mic). **d** Top 30 enriched pathways in SenMayo-hi Mic with senescence-related pathways highlighted in blue (FDR < 0.01). See the Supplementary Table 4b for a full list. **e** Violin plots depicting increased expression of genes related to AP1 pathway, IL4/13 and IL10 signalling in SenMayo-hi Mic.

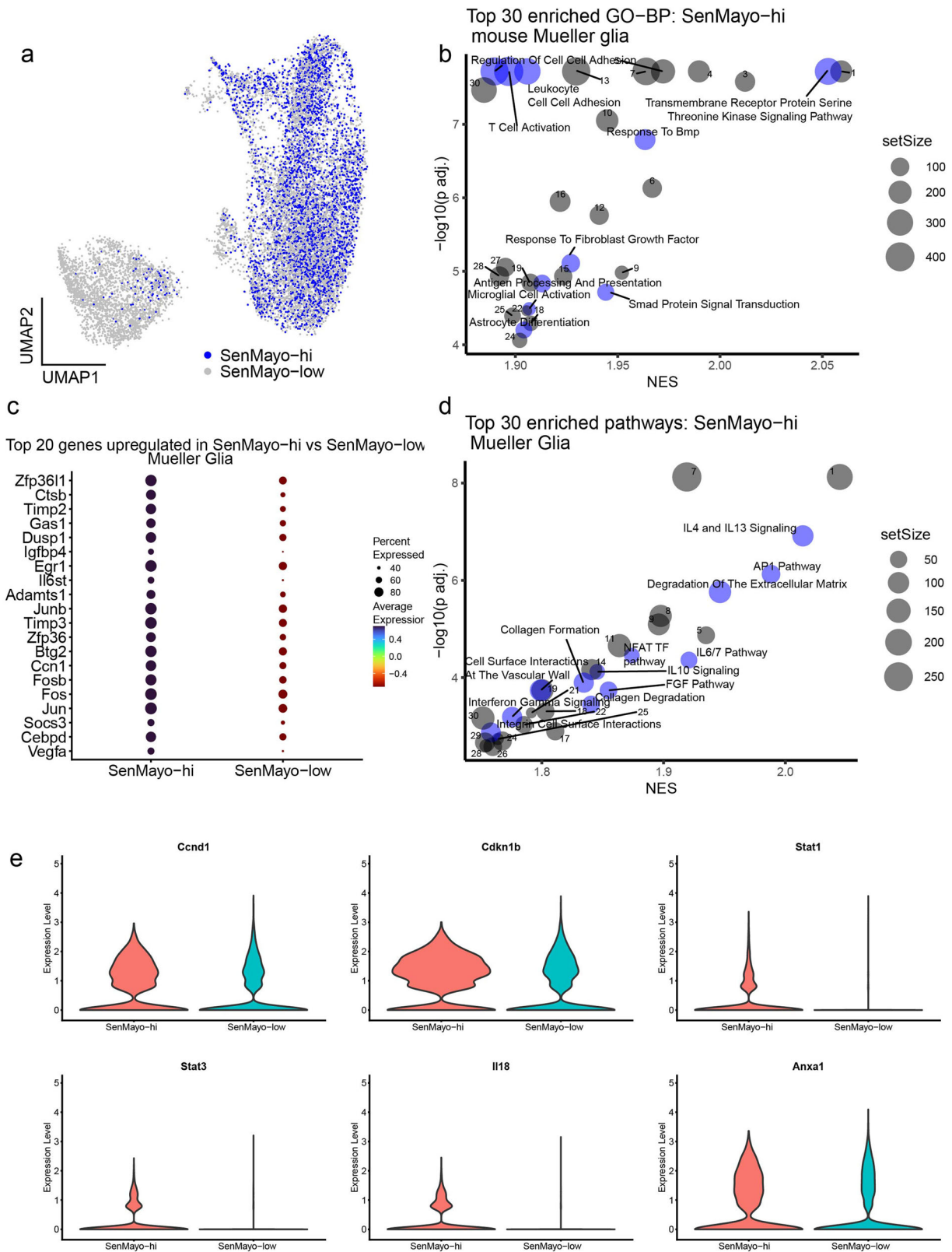


Fig. 3 | SenMayo-hi cells detected in the retinal Mueller glia (MG). **a** UMAP plot of SenMayo-hi cells in the MG subcluster. **b** Top 30 enriched biological processes (BP) in SenMayo-hi MG with senescence and glial response processes highlighted in blue (FDR < 0.01). See the Supplementary Table 6a for a full list. **c** Top 20 genes upregulated in the SenMayo-hi MG (vs SenMayo-low MG). **d** Top 30 enriched pathways

in SenMayo-hi MG with senescence-related pathways highlighted in blue (FDR < 0.01). See the Supplementary Table 6b for a full list. **e** Violin plots depicting increased expression of genes related to AP1 pathway and interleukin 4/13 signalling in SenMayo-hi MG.

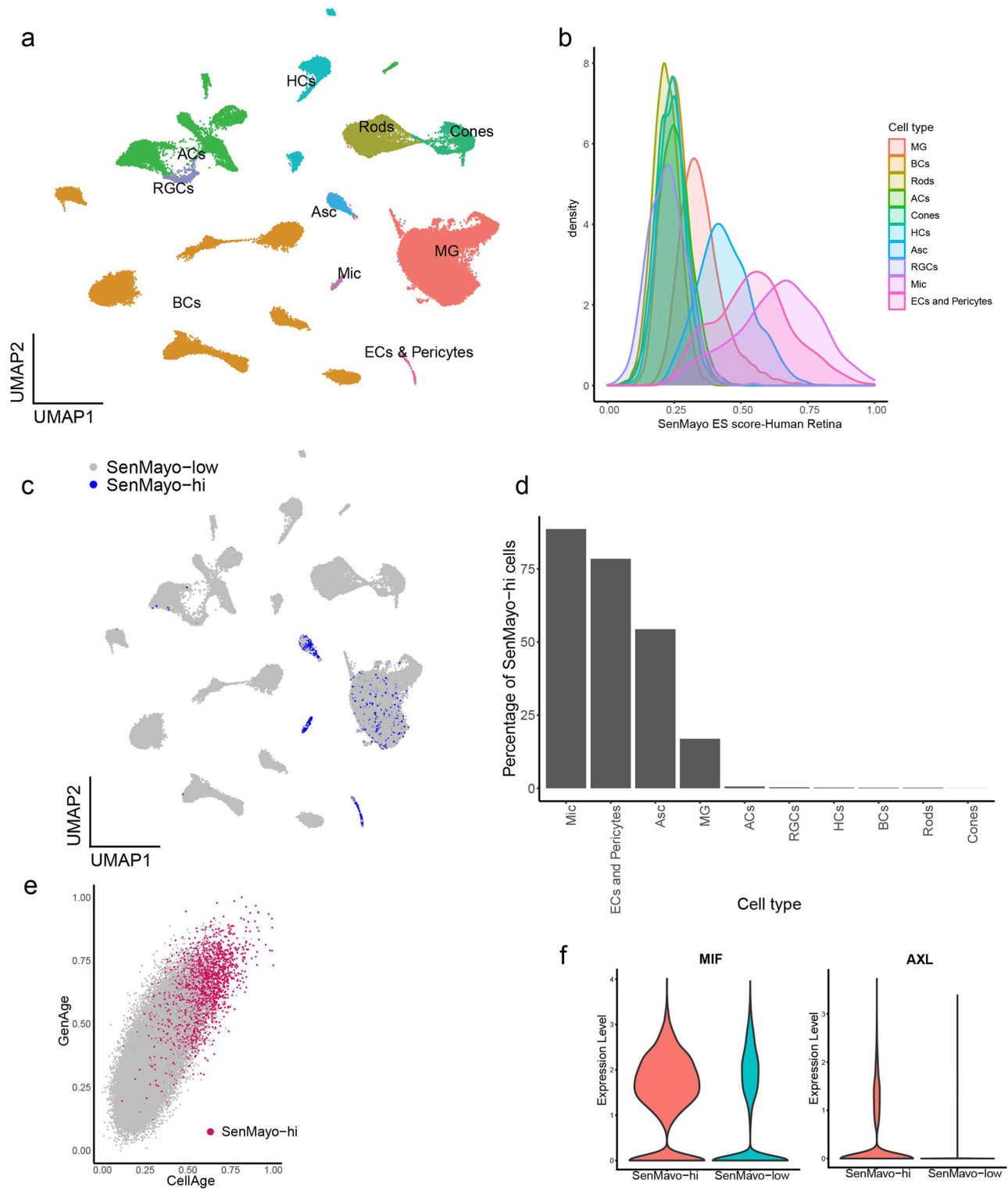


Fig. 4 | Microglia and other glial cells comprise most of the SenMayo-hi cells in the human retina. **a** UMAP plot depicting cell types in the human retina⁵⁹ (GEO: GSE148077). Cells detected include Rods, Cones, Retina Ganglion cells (RGCs), Bipolar cells (BCs), Amacrine cells (ACs), Horizontal cells (HCs), Mueller glia (MG), Astrocytes (Asc), Microglia (Mic) and Endothelial cells & Pericytes (ECs and

Pericytes). **b** SenMayo enrichment score (ES) distribution in the human retina by cell type. **c** UMAP plot of human retina depicting SenMayo-hi cells. Mic cells score the highest. **d** Percentage of SenMayo-hi cells in different cell types in the human retina. **e** SenMayo-hi cells also score high for GenAge and CellAge gene sets. **f** Violin plots show the upregulation of MIF and AXL in SenMayo-hi cells in the human retina.

Interleukin and AP1 signalling pathways are conserved in mouse and human SenMayo-hi retinal microglia

Comparison of gene expression changes of SenMayo-hi glial cells (microglia and Mueller glia) in human and mouse retina showed a good correlation of

DEGs (Fig. 5a, b). In retinal microglia, apart from some AP1 transcription factor genes that were upregulated in both human and mouse, we identified genes such as *Gpr183*⁶⁰, *Cited2*⁶¹, *Mcl1*⁶² and *Cd83*⁶³ that are involved in senescence and inflammatory regulation (Fig. 5a). Similarly in the Mueller

glia, a number of genes upregulated in both mouse and human SenMayo-hi cells, were positive and negative regulators of senescence, several of which were related to the ECM maintenance⁶⁴ such as *Mmp14*, *Adamts1* and *Sparc*^{65–68} (Fig. 5b).

Pathways that were commonly enriched in SenMayo-hi microglia across species included key interleukin signalling pathways such as IL4/13, IL10 and AP1 signalling (Fig. 5c, Supplementary Table 4b, 7a), which were also enriched in the SenMayo-hi retinal microglia from the Saban lab dataset (Supplementary Table 12). SenMayo-hi human and mouse Mueller glia and SenMayo-hi human astrocytes also showed enrichment for IL4/13 and IL10 signalling (Fig. 5d, Supplementary Fig. 5a, Supplementary Table 6b, 7b, 7c). Other pathways which can promote senescence and are conserved in microglia across species are NFAT pathway^{49,69} and FRA pathway⁷⁰ (Fig. 5c, Supplementary Table 7a).

Since some microglial AP1 pathway genes have been implicated to be activated during tissue dissociation⁷¹, we re-ran these genes from the list of all genes expressed in retinal microglia in our dataset, human retina and Saban mouse retinal microglia and re-ran the GSEA pathway analysis and did not detect any significant changes to our previous results. Both AP1 pathway and interleukin 4/13 and 10 signalling were still highly enriched in the SenMayo-hi microglia of these datasets (Supplementary Table 13).

Cell-cell communication pathways were also conserved in mouse (Fig. 5e, Supplementary Fig. 5b, d) and human (Fig. 5f, Supplementary Fig. 5c, e) retinal SenMayo-hi cells. These include the amyloid precursor pathway (APP) which shows ligand-receptor (L-R) interaction from SenMayo-hi Mueller glia and astrocytes to SenMayo-hi microglia and the prosaposin pathway (PSAP) which communicates from SenMayo-hi Mueller glia/astrocytes and microglia to SenMayo-low Mueller glia (Supplementary Fig. 5d, e).

Impact of advancing age on the SenMayo panel expression

In both the human and mouse datasets we focussed on the SenMayo-hi glia cells to determine whether there was an increase in SenMayo enrichment score with age. In our dataset (Fig. 6a) as well as in the two independent retinal datasets (Saban lab- Supplementary Fig. 6a, b, Chen lab, mouse retina atlas, Supplementary Fig. 6c, d), there was no increase in SenMayo enrichment scores with age in the mouse microglia. Similarly, no trend was observed in mouse Mueller glial cells with age (Fig. 6b). In addition, none of the retinal neurons showed an increase in SenMayo enrichment score with age (Supplementary Fig. 7). In comparison, human retinal samples showed significant increase of senescent cells with age. SenMayo-hi human microglial cells show a significant increase in SenMayo enrichment scores with age (Fig. 6c), while Mueller glia shows a significant increase of senescent scores in cells derived from both the 60 and 70 age group in comparison to the cells derived in the 50 s age group (Fig. 6d). *CCL4*, *CXCL8*, *IL1B*, *ICAM1* are among the SenMayo genes driving the age-related increase of senescence scores in human retina microglia (Fig. 6e) and *JUN*, *IGFBP5*, *DKK1*, *GEM* and *CXCL12* appear to be increasing with age in Mueller glia (Fig. 6f). We also evaluated the link between ageing and senescence gene expression in other mouse tissues using public single-cell mouse datasets. As observed in the retina, brain microglia also score highly for the SenMayo panel, as observed in an ageing mouse brain dataset from the Peng lab (Supplementary Fig. 6e). Unlike retinal microglia, brain microglia show a significant increase in SenMayo scores at 24 months of age (Supplementary Fig. 6f). This is more evident in another ageing brain microglia series comprising 3-, 14- and 24-month samples (Supplementary Fig. 6g, h). To understand the relevance of SenMayo enrichment with ageing in non-CNS tissue, we analysed various other mouse non-CNS datasets. In mouse livers, Kupffer cells, the resident macrophage, scored highest for SenMayo enrichment scores (Supplementary Fig. 6i) showing a significant increase in SenMayo enrichment scores in Kupffer cells only from 30mo livers compared to even 24-month livers (Supplementary Fig. 6j). In accordance with the literature⁷², mouse adipose tissue did not show and age-related enrichment of senescence (Supplementary Fig. 6k,l).

To analyse other age-related changes in different mouse retinal cell types, we performed differential gene expression analysis in various retinal cell types (rods, Mueller glia, cones and bipolar cells), comparing 12- and 24-month cells to 3-month cells. IPA analysis of the DEGs was conducted (Fig. 7, Supplementary Tables 8–11). Reduction of synaptic signalling pathways was apparent, especially in the bipolar cells (e.g., glutaminergic and adrenergic), but also general synaptic long-term depression in the rods and cones, and Mueller glia pathways pointed towards reduction of neuroprotective and regenerative potential of Mueller glia as well as with age^{73,74}.

Discussion

In summary, our study explored gene expression data using single-cell RNA-seq to identify the signatures of senescence in mouse retina during normal ageing. We additionally compared transcriptomic datasets for the mouse and human retina using the recently published SenMayo transcriptomics panel. Both retinal microglial and macroglial cells (Mueller glia and astrocytes) were highly enriched for the SenMayo senescence gene panel. Our age-related analysis showed an increase of retinal glial senescence during ageing in the human retina, which was not apparent in the mouse retina up to age 24 months but interestingly was present in the ageing murine brain microglia. Interleukin signalling via IL 4, 13 and 10 signalling and the AP1 pathway were identified as conserved pathways in the senescent glial cells in mouse and human retina.

As in the rest of the CNS, glial cells play a major role in retinal health and homeostasis. Microglial cells with support of the macroglia cells are the major components of the retinal immune system^{75–77}. Transcriptomic signatures of senescence in microglial and to a slightly lesser extent in macroglial cells increased in the ageing human retina and murine brain, however not in the murine retina. The increase of senescent microglia in the ageing brain has been demonstrated previously and has been postulated to be a major contributor to age-related neurodegenerative diseases, and thus potential therapeutic targets^{78–82}. In comparison to the brain, microglial senescence in the retina has been less well studied. Retinal microglia show age-related changes in motility and morphology which has been discussed in the context of the senescence of these cells⁸³ and senescence-related human microglial signatures have been linked to age-related macular degeneration⁸⁴. Recent studies demonstrate significant differences in scSeq signatures between the murine brain and retinal microglia. Retinal microglia exhibited a more pro-inflammatory signature than brain microglia, which could explain opposing effects of the same microglial signals in the brain and the retina⁸⁵. Human and murine microglial signals are largely conserved⁸⁶, however, as microglia are highly dependent on their microenvironment, differences in senescence signatures with age could potentially be enhanced in humans living in non-controlled environments and potentially unhealthy lifestyle choices in comparison to healthy laboratory mice subjected to the standardised environment.

Interestingly, clear evidence of SenMayo-hi senescent transcriptomics was seen in the microglia and macroglia of the retina - and the brain - of young mice. As many inflammatory markers released by microglial and macroglial cells overlap with the SASP signature, inflammatory changes could provide an alternative explanation for the detection of SenMayo-hi glial cells across all ages. We do however also detect enrichment of SenMayo gene panel independent senescence markers including *Tgfb2*^{25,87,88} in our SenMayo-hi cells and further senescence hallmarks such as enrichment of cell cycle arrest genes and a shift towards replicative arrest in SASP-rich cells detected as senescent by the SenMayo panel have been previously demonstrated, strengthening the likelihood that these cells are truly senescent⁶. As senescent cells also hold beneficial roles in various tissues and circumstances such as enhancement of cell plasticity or adaptive processes, this could explain the presence of senescent cells in younger tissues. However, this aspect of senescence is currently still widely understudied and needs to be researched in greater detail^{89–91}. Other than paracrine signalling for example via SASP, autocrine signalling is a well-described phenomenon in senescent cells. This was also apparent in the senescent retinal microglia and macroglia. Looking more specifically into genes and pathways regulated in the

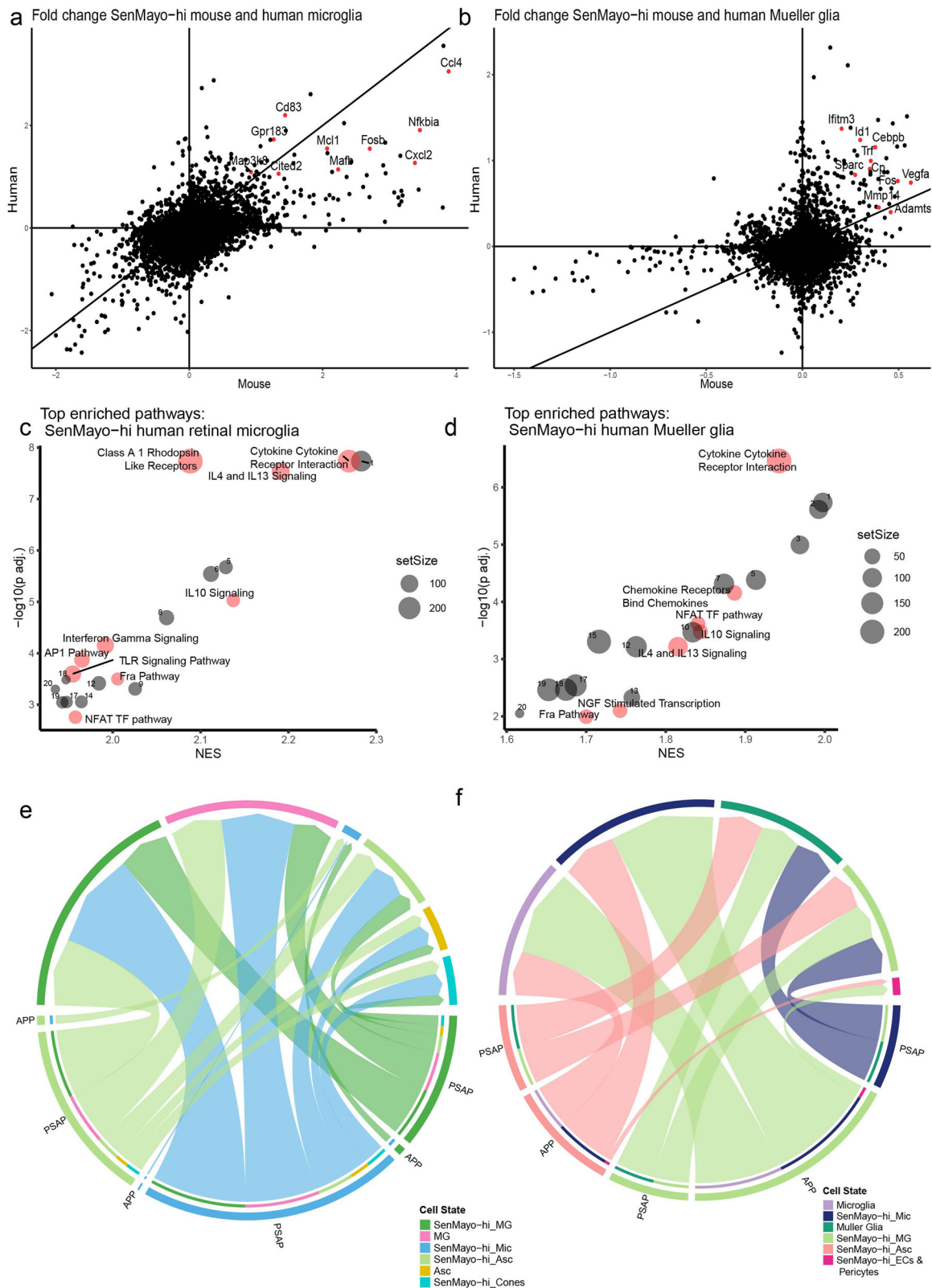


Fig. 5 | Comparison of SenMayo-hi glia in mouse and human retina datasets shows conserved interleukin signalling in all glial cells and AP1 pathway enrichment in microglia specifically. **a** Scatter plot comparing log fold change of genes in SenMayo-hi microglia (Mic) (against SenMayo-low Mic) in mouse and human retina. **b** Scatter plot comparing log fold change of genes in SenMayo-hi Mueller glia (MG) in mouse and human retina (against SenMayo-low Mueller glia). **c** Dotplot of enriched pathways in human SenMayo-hi Mic with pathways that are

also enriched in mouse Mic highlighted and labelled in red (FDR < 0.01) See Supplementary Table 9a for a full list. **d** Dotplot of enriched pathways in human SenMayo-hi MG with pathways that are also enriched in mouse MG highlighted and labelled in red (FDR < 0.01) See Supplementary Table 9b for a full list. **e** and **f** Selected common interaction pathways in mouse and human SenMayo-hi cells include APP and PSAP pathways. In both **e** mouse and **f** human many interactions of SenMayo-hi cells include signalling to other SenMayo-hi glia.

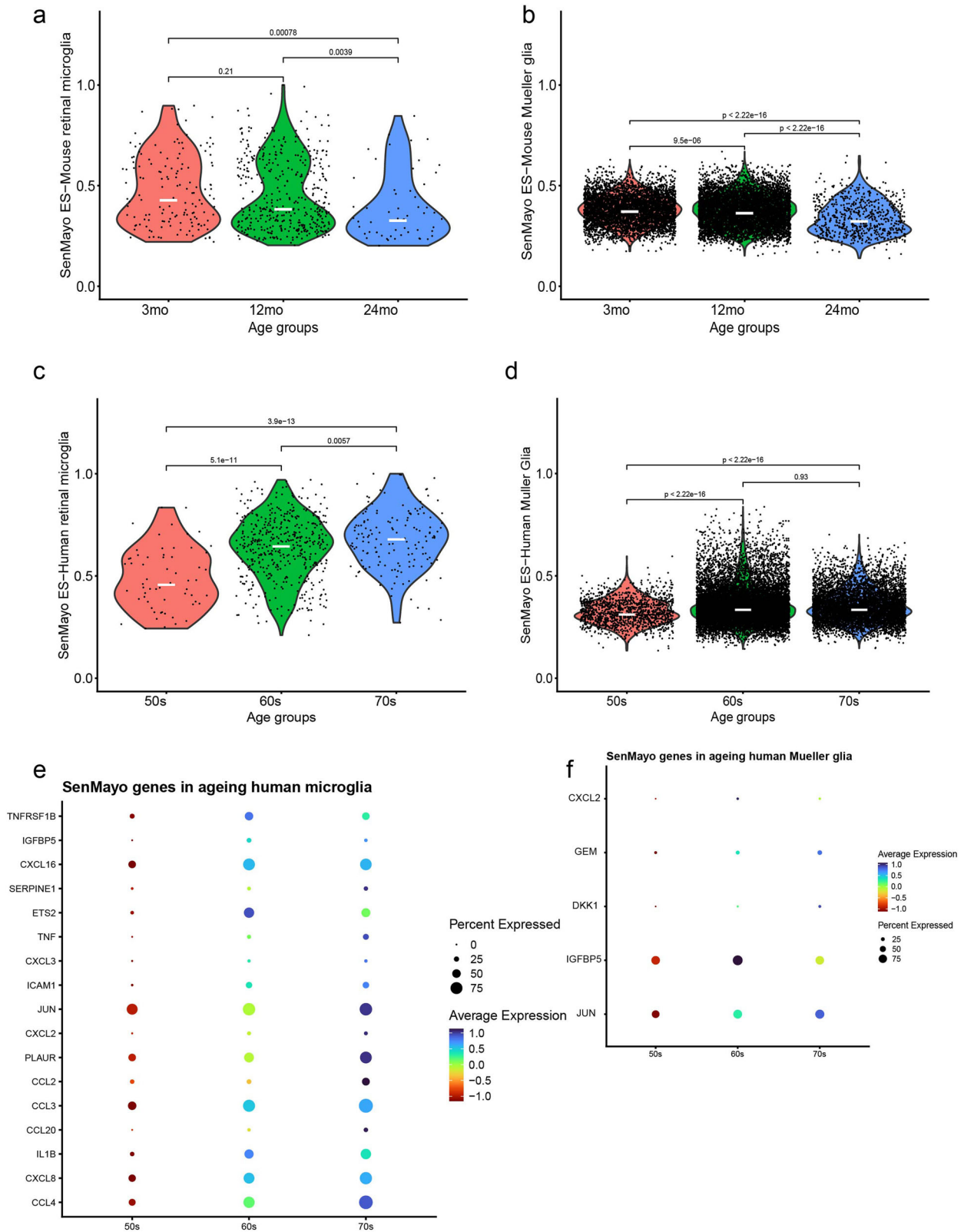


Fig. 6 | SenMayo panel enrichment with age in the retina. SenMayo enrichment scores (ES) in the **a** mouse microglia and **b** mouse Mueller glia clusters show no trend to increase with age. Increased SenMayo enrichment scores with age in **c** human

microglia (significant increase) **d** Mueller glia (significant increase between both 60 s and 70 s vs 50 s). SenMayo genes that are increased with age in **e** human microglia and **f** Mueller glia.

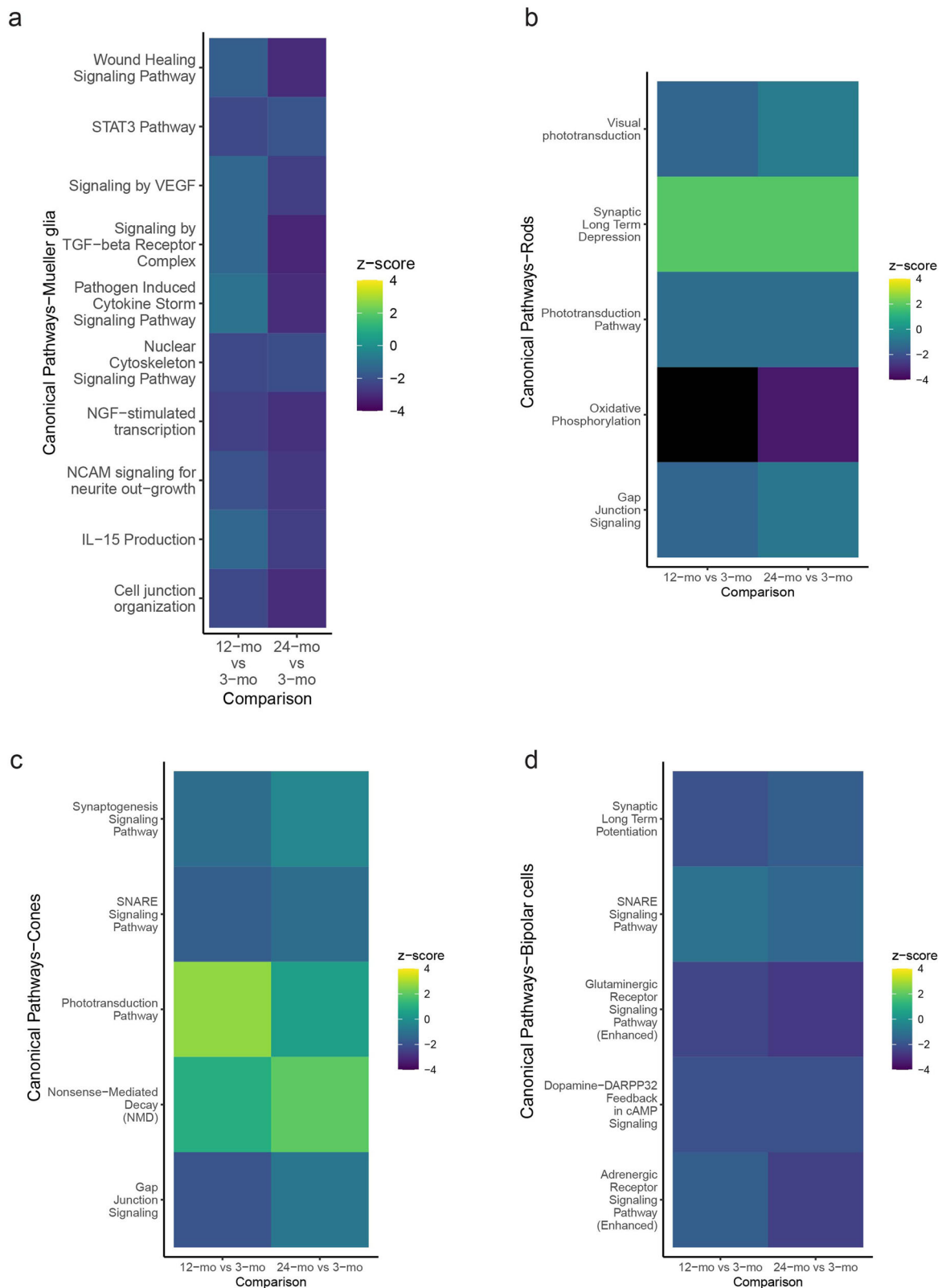


Fig. 7 | Age-related changes in the mouse retina. IPA canonical pathway comparison analysis of DEGs from 12-mo vs 3-mo and 24-mo vs 3-mo **a** Mueller glia, **b** rod photoreceptors **c** cone photoreceptors and **d** Bipolar cells (p -value < 0.05).

SenMayo-hi senescent glial cells in our datasets, we identified that IL-4/13 and IL-10 signalling and respective up and downstream molecules were enriched in all the analysed senescent glial cells- microglia and Mueller glia from the retina and brain microglia. Next to their relevance in inflammation, IL-4,10 and 13 are known to drive senescence in various contexts and

cell types^{35,50,51,92-97}. AP1 pathway, and in particular Jun and Fos family members, was enriched in both the mouse and human senescent SenMayo-hi microglial cells in both the retina and the brain. In brain microglia, the AP1 pathways are not only activated with ageing but also promote accelerated microglial activation after injury⁹⁸. It is regarded as a key

transcriptional driver of senescence³⁷ and downstream elements such as *Cdkn1b* (p27) and *CyclinD1*, both upregulated in the SenMayo-hi senescent retinal glial cells, are known to be upregulated in senescent cells and also promote senescence^{52,53,99–101}. The AP1 family can not only drive cellular senescence such as oncogenic and replicative senescence^{37,38} but also plays a role in inflammation, where an upregulation of the AP1 family members *Jun* and *Fos* has been observed¹⁰². Interestingly, co-expression analysis of the SASP cluster in the original paper characterising the SenMayo Panel revealed a strong correlation between *JUN* and classical senescence marker *CDKN2A/p16^{INK4a}* and therefore suggests this gene as a potential marker for senescence⁵. A recent meta-analysis identified key pathways and proteins related to different stages of senescence and senescence stressor types³⁵. Enrichment of pathways such as AP1³⁸, IL4/13³⁵ and pathways related to ECM reorganisation³⁵ in SenMayo-hi glia in the retina potentially implies that they are in the late stage of senescence and replicative senescence is the potential stressor involved. With the growing interest in retinal ageing and retinal transcriptomics, we could perform such comparative analyses of senescence signatures in the retina in future.

Potential weaknesses exist with regard to this analysis. We only aged mice to 24 months of age and senescence may increase more rapidly above this age in the retina. Our analysis of liver Kupffer cells revealed that SenMayo panel scores were significantly higher in 30-mo mice compared to 24-mo animals, and future analysis of older mouse retina would be necessary to determine if a similar acceleration in senescence is seen observed. Studies show that brain microglial cell single-cell transcriptomics analysis can be particularly sensitive to variations in experimental preparation procedures, which can influence the transcription levels of various intermediate early genes such as *Jun*, *Fos*, *Egr1*⁷¹. Removing these genes from the SenMayo panel had no influence on our results, however, this aspect should be taken into consideration when analysing microglial transcriptomics and when comparing different datasets. We further acknowledge that future mechanistic investigations are necessary to better our understanding of IL-4,13, IL10 and AP1 pathways and their role in retinal glial senescence.

With this early look into the ageing retinal panel, we show that the SenMayo panel allows transcriptomic evidence of senescent microglia and macroglial cells in the human and mouse retina and shows an apparent increase in glial senescence in the human retina with age. Interleukins 4, 10 and 13 appear to be relevant players in retinal glial senescence and the AP1 pathway in retinal microglial senescence is also implicated across species. Application of the SenMayo gene sets to future human glaucoma single-cell datasets and mouse retinal injury models could possibly help parse the link between this disease and senescence established by GWAS studies.

Materials and methods

Animal strain and husbandry

All animal procedures conformed to the ARVO Statement for the Use of Animals in Ophthalmic and Vision Research and were approved by the SingHealth Institutional Animal Care and Use Committee (2019/SHS/1534). Male and female C57BL/6J mice (NNT mutation-positive) at 3 and 12 months of age were purchased from InVivos Pte Ltd, Singapore, and housed at the SingHealth Experimental Medicine Centre (Academia, Singapore) in a temperature- (22 ± 1 °C), light- (12 h light, 12 h dark) and humidity-controlled (30–40%) environment with free access to food and water. Mice were aged from 12 months to 24 months of age within the Animal facility of SingHealth Experimental Medicine Centre.

Single-cell isolation

2 non-injured retinas were collected from C57BL/6J mice per condition. Retinal tissue was digested using the papain dissociation system (Worthington) following the manufacturer's protocol. Cells were passed through a 30 µm filter (Miltenyi) to obtain a single-cell suspension. Following this different magnetic activated cell sorting methods (MACS®) enrichment/depletion methods were used on the cell pool collected. ACSA-2 and Thy1.2 enrichment: Cell pool was enriched for RGCs and macroglia using Thy1.2 and ACSA-2 (astrocyte cell surface antigen-2) antibodies respectively. Two

retinas from 2 mice per age group were pooled for this method - 3-month (young), 12-month (middle-aged) and 24-month-old (old). CD73 depletion: The cell pool was depleted of rod photoreceptors using the CD73 antibody. Retinae from four 12-mo mice were prepared this way (2 retinas per pooled for each replicate). Thy1.2 enrichment and CD73 depletion: Cell pool was split into two halves and each half was subjected to either Thy1.2 enrichment or CD73 depletion. Following this, the two portions were combined again. Two retinas from 2 mice per age group were used for this method - 3-mo and 12-mo.

Single-cell sequencing

10,000 cells per sample were loaded onto Chromium Next GEM Single-Cell 3' Kit v3.1 (10x Genomics), and libraries were generated in-house using the Chromium Controller (10x Genomics). Sample QC was performed at relevant steps following the manufacturer's protocols. The samples were sequenced on the Illumina HiSeq150 platform. FASTQ files were aligned to the mouse transcriptome mm10 with the counts function of 10x Genomics Cell Ranger 6.0.2 and analysis of the filtered counts was performed with Seurat v4 (4.1.1)¹⁰³.

Analysis of in-house transcriptomics data

The dataset comprising 2 replicates for 3-mo, 4 replicates for 12-mo and 1 replicate for 24-mo retina was integrated using the Seurat canonical correlation analysis (CCA) method. After quality control of the merged datasets, the following cells were retained: percent.mt <50% & >200 nFeature_RNA & <3500 nFeature_RNA^{104,105} (Supplementary Fig 1). Log normalisation was performed with the scale factor set as 10,000 (default Seurat settings) following which 2000 highly variable features were identified. Integration was performed and 50 principal components (PCs) were used for clustering (k nearest neighbours graph-based clustering) and dimensional reduction via uniform manifold projection (UMAP) was performed. Clustree package (v0.4.4) was used for optimal cluster resolution¹⁰⁶ (Supplementary Fig 1f, g). We annotated the cells using an established panel of retinal cell type markers (Fig. 1a, Supplementary Table 1)¹⁰⁷.

After clustering and annotating for cell type, we performed gene set enrichment analysis (GSEA) using the *enrichIT* function of the R package *escape* (v1.9.0)¹⁰⁸ for the following datasets- SenMayo⁶ (mouse), GenAge, CellAge^{22,23,109}, Cherry_2023²⁶ and SenMayo panel without microglial genes (SenMayo-reduced) (Supplementary Table 2). GenAge was published in 2009 based on a meta-analysis of 127 publicly available microarray and RNA-Seq datasets from mice, rats and humans²³ whereas CellAge was manually curated based on data derived from gene-manipulation studies in various human cell types²². The 862 gene containing Cherry_2023 panel was derived from a murine foreign body driven fibrosis model in p16 expressing cells²⁶. For our analysis, we used the genes derived from the differential gene expression analysis derived from the bulk RNA sequencing performed by the authors and chose those genes upregulated in the p16+ stroma with a false discovery rate (FDR) of <0.05. To ensure that the panel is not falsely detecting microglial cells, we created a SenMayo-reduced dataset which was derived by removing all genes from the SenMayo panel that were part of the HU_FETAL_RETINA_MICROGLIA gene set (M39266) from Molecular Signatures Database (MSigDB)^{27,110,111}. These datasets served as independent controls. All gene lists used can be found in Supplementary Table 2. The enrichment scores for the SenMayo gene panel were calculated and to determine which cells scored highest, we plotted density graphs (Fig. 1b). We observed that the SenMayo score distribution in the microglial cells was the highest, they were used to set the threshold for SenMayo-hi scoring cells. The *mixtools* (v2.0.0)¹¹² R package was used to resolve the bimodal distribution of SenMayo enrichment scores in the microglial cluster (Supplementary Fig. 2a, b). We determined the intersection point of the two clusters as threshold by which cells were either classified as SenMayo-hi or SenMayo-low (Fig. 1c), which then led to a high correlation of the SenMayo-hi cells with the independent ageing control panels (Fig. 1e). After calculating fold changes of all expressed genes in different comparisons using Seurat "FoldChange", the results were passed onto the package

clusterProfiler (v4.2.2)¹¹³ to perform GSEA using the MSigDB collection to identify pathways and gene ontology biological processes and terms with FDR of <0.01 were retained. Top 30 terms (based on normalised enrichment score-NES) were depicted as a dotplot. Differentially expressed genes (LFC of 0.25 and *p*-value-adj <0.01) were identified with Seurat “FindMarkers”. Cell-cell communication was determined with CellChat package (v1.6.1)¹¹⁴. To account for the possible effect of cell dissociation on microglial gene expression, we removed genes that were identified to be upregulated during this process⁷¹ and re-ran GSEA pathway analysis. To determine age-related changes in different retinal cell types, the various cell types were subsetted, “RunPCA” and “RunUMAP” (using 30 PCs) were performed. Differential gene expression change was calculated by comparing both the 12-mo and 24-mo age group to the 3-mo age group which served as the control using Seurat “FindMarkers” (|LFC| of 0.25 and *p*-value-adj <0.01). IPA (Ingenuity Pathway Analysis- QIAGEN Inc., <https://digitalinsights.qiagen.com/IPA>)¹¹⁵ was performed with the DEGs from the various cell types and pathway comparison analysis was then performed across ages.

Data retrieval and analysis of publicly available retina datasets

We downloaded the human retinal dataset count files from the GSE148077 dataset deposited within the Gene-Expression Omnibus (GEO) database and analysed this using the same QC parameters as applied for the mouse retinal dataset (Supplementary Fig. 3). The human retinal dataset comprised of 7 donor samples ranging from 53–78 years of age without reported ocular disease. The cause of death was cancer-related in all but one of the donors, where the given cause of death was due to interstitial lung disease. One of the donors was female, all other donors were male. Foveal tissue was analysed from 5 donors, only the peripheral retina for one donor and both the foveal and peripheral retina for another donor. Time from death to tissue process was less than 6.5 h for all but one donor⁵⁹. We grouped the samples according to age resulting in 3 age groups- 50 s (53yo), 60 s (60, 64, 65, 69yo) and 70 s (74, 78yo) for our age-related analysis of senescence. The datasets were integrated via canonical correlation analysis (CCA) method and 30 PCs were used for clustering and UMAP. A known panel of retinal cell type markers was used to annotate the cells¹⁰⁷.

The mouse retinal immune feature barcode matrices were downloaded from the GSE195891 dataset deposited in the GEO database (Supplementary Fig. 6a). After retaining the 2-mo and 24-mo samples, quality control was performed with the parameters used in the original paper: nFeature_RNA >200 & nFeature_RNA <5000 & percent.mt <20¹¹⁶.

The Chen lab mouse retinal atlas was downloaded from the CZ CELLX GENE repository (Supplementary Fig. 2g)¹¹⁷.

Mouse adipose (Supplementary Fig. 6k) and liver (Supplementary Fig. 6i) datasets were downloaded from the Tabula Muris Senis repository¹¹⁸. Brain microglia (GSE207932) and whole brain (GSE208292) datasets from the Peng lab were retrieved from the GEO database¹¹⁹. The escape package was used on all public datasets to obtain gene set enrichment scores for various gene panels.

Statistical analysis

R software (v4.1.0) was used for statistical analysis. For differentially expressed genes in the scRNA seq analysis, the Wilcoxon rank-sum test, with Bonferroni correction (default for Seurat “FindMarkers”) was used and a cut-off of adjusted *p*-value < 0.01 was set.

To compare the SenMayo enrichment score in various cell types, a two-tailed Wilcoxon rank-sum test was performed, and *p*-values < 0.05 were considered significant.

Data availability

The datasets generated and/or analysed during the current study are available in the Gene Expression Omnibus repository (GEO) repository (GSE268463).

Received: 21 May 2024; Accepted: 18 November 2024;

Published online: 30 November 2024

References

- Hayflick, L. & Moorhead, P. S. The serial cultivation of human diploid cell strains. *Exp. Cell Res.* **25**, 585–621 (1961).
- Kumari, R. & Jat, P. Mechanisms of cellular senescence: cell cycle arrest and senescence associated secretory phenotype. *Front. Cell Dev. Biol.* **9**, 645593 (2021).
- Campisi, J. Aging, cellular senescence, and cancer. *Annu. Rev. Physiol.* **75**, 685–705 (2013).
- Herranz, N. & Gil, J. Mechanisms and functions of cellular senescence. *J. Clin. Invest.* **128**, 1238–1246 (2018).
- Campisi, J. & D’Adda Di Fagagna, F. Cellular senescence: when bad things happen to good cells. *Nat. Rev. Mol. Cell Biol.* **8**, 729–740 (2007).
- Saul, D. et al. A new gene set identifies senescent cells and predicts senescence-associated pathways across tissues. *Nat. Commun.* **13**, 4827 (2022).
- López-Otín, C., Blasco, M. A., Partridge, L., Serrano, M. & Kroemer, G. The hallmarks of aging. *Cell* **153**, 1194 (2013).
- Dimri, G. P. et al. A biomarker that identifies senescent human cells in culture and in aging skin in vivo. *Proc. Natl Acad. Sci. USA* **92**, 9363–9367 (1995).
- Baker, D. J. et al. Clearance of p16 Ink4a-positive senescent cells delays ageing-associated disorders. *Nature* **479**, 232–236 (2011).
- Atella, V. et al. Trends in age-related disease burden and healthcare utilization. *Aging Cell* **18**, e12861 (2019).
- Guerreiro, R. & Bras, J. The age factor in Alzheimer’s disease. *Genome Med.* **7**, 1–3 (2015).
- Reeve, A., Simcox, E. & Turnbull, D. Ageing and Parkinson’s disease: why is advancing age the biggest risk factor? *Ageing Res. Rev.* **14**, 19–30 (2014).
- Kapetanakis, V. V. et al. Global variations and time trends in the prevalence of primary open angle glaucoma (POAG): a systematic review and meta-analysis. *Br. J. Ophthalmol.* **100**, 86–93 (2016).
- Ehrlich, R. et al. Age-related macular degeneration and the aging eye. *Clin. Interv. Aging* **3**, 473–482 (2008).
- Jurk, D. et al. Postmitotic neurons develop a p21-dependent senescence-like phenotype driven by a DNA damage response. *Aging Cell* **11**, 996–1004 (2012).
- Sapieha, P. & Mallette, F. A. Cellular senescence in postmitotic cells: beyond growth arrest. *Trends Cell Biol.* **28**, 595–607 (2018).
- Sikora, E. et al. Cellular senescence in brain aging. *Front. Aging Neurosci.* **13**, 646924 (2021).
- Skowronska-Krawczyk, D. et al. P16INK4a upregulation mediated by SIX6 defines retinal ganglion cell pathogenesis in glaucoma. *Mol. Cell* **59**, 931–940 (2015).
- Binet, F. et al. Neutrophil extracellular traps target senescent vasculature for tissue remodeling in retinopathy. *Science* **369**, eaay5356 (2020).
- Crespo-Garcia, S. et al. Pathological angiogenesis in retinopathy engages cellular senescence and is amenable to therapeutic elimination via BCL-xL inhibition. *Cell Metab.* **33**, 818–832.e7 (2021).
- Terao, R. et al. Cholesterol accumulation promotes photoreceptor senescence and retinal degeneration. *Invest. Ophthalmol. Vis. Sci.* **65**, 29 (2024).
- Avelar, R. A. et al. A multidimensional systems biology analysis of cellular senescence in aging and disease. *Genome Biol.* **21**, 91 (2020).
- de Magalhães, J. P., Curado, J. & Church, G. M. Meta-analysis of age-related gene expression profiles identifies common signatures of aging. *Bioinformatics* **25**, 875–881 (2009).
- Tominaga, K. & Suzuki, H. I. TGF- β signaling in cellular senescence and aging-related pathology. *Int. J. Mol. Sci.* **20**, 5002 (2019).
- Yu, A. L., Birke, K., Moriniere, J. & Welge-Lüssen, U. TGF- β 2 induces senescence-associated changes in human trabecular meshwork cells. *Invest. Ophthalmol. Vis. Sci.* **51**, 5718–5723 (2010).

26. Cherry, C. et al. Transfer learning in a biomaterial fibrosis model identifies in vivo senescence heterogeneity and contributions to vascularization and matrix production across species and diverse pathologies. *GeroScience* **45**, 2559–2587 (2023).
27. Hu, Y. et al. Dissecting the transcriptome landscape of the human fetal neural retina and retinal pigment epithelium by single-cell RNA-seq analysis. *PLoS Biol.* **17**, e3000365 (2019).
28. Gonzalez-Meljem, J. M., Apps, J. R., Fraser, H. C. & Martinez-Barbera, J. P. Paracrine roles of cellular senescence in promoting tumorigenesis. *Br. J. Cancer* **118**, 1283–1288 (2018).
29. Kim, N. Y., Woo, A. M., Kim, J. R. & Lee, C. Exploration of senescence-associated genes by differential display reverse transcription polymerase chain reaction: Prosaposin as a novel senescence-associated gene. *Arch. Pharm. Res.* **32**, 737–745 (2009).
30. Ross-Munro, E. et al. Midkine: the who, what, where, and when of a promising neurotrophic therapy for perinatal brain injury. *Front. Neurol.* **11**, 568814 (2020).
31. Feng, D. C. et al. Identification of senescence-related molecular subtypes and key genes for prostate cancer. *Asian J. Androl.* **25**, 223–229 (2023).
32. Bejjani, F., Evanno, E., Zibara, K., Piechaczyk, M. & Jariel-Encontre, I. The AP-1 transcriptional complex: local switch or remote command? *Biochim. Biophys. Acta Rev. Cancer* **1872**, 11–23 (2019).
33. Kolesnichenko, M. et al. Transcriptional repression of NFKBIA triggers constitutive IKK- and proteasome-independent p65/RelA activation in senescence. *EMBO J.* **40**, e104296 (2021).
34. Chen, D. et al. LncRNA NEAT1 suppresses cellular senescence in hepatocellular carcinoma via KIF11-dependent repression of CDKN2A. *Clin. Transl. Med.* **13**, e1418 (2023).
35. Oguma, Y. et al. Meta-analysis of senescent cell secretomes to identify common and specific features of the different senescent phenotypes: a tool for developing new senotherapeutics. *Cell Commun. Signal.* **21**, 262 (2023).
36. Maciel-Barón, L. A. et al. Senescence associated secretory phenotype profile from primary lung mice fibroblasts depends on the senescence induction stimuli. *Age* **38**, 1–14 (2016).
37. Martínez-Zamudio, R. I. et al. AP-1 imprints a reversible transcriptional programme of senescent cells. *Nat. Cell Biol.* **22**, 842–855 (2020).
38. Wang, Y., Liu, L., Song, Y., Yu, X. & Deng, H. Unveiling E2F4, TEAD1 and AP-1 as regulatory transcription factors of the replicative senescence program by multi-omics analysis. *Protein Cell* **13**, 742–759 (2022).
39. Muela-Zarzuola, I. et al. NLRP1 inflammasome promotes senescence and senescence-associated secretory phenotype. *Inflamm. Res.* **73**, 1253–1266 (2024).
40. Zhou, P., Wan, X., Zou, Y., Chen, Z. & Zhong, A. Transforming growth factor beta (TGF- β) is activated by the CtBP2-p300-AP1 transcriptional complex in chronic renal failure. *Int. J. Biol. Sci.* **16**, 204–215 (2020).
41. Vartanian, R. et al. AP-1 regulates cyclin D1 and c-MYC transcription in an AKT-dependent manner in response to mTOR inhibition: Role of AIP4/Itch-mediated JUNB degradation. *Mol. Cancer Res.* **9**, 115–130 (2011).
42. Saraiva, M., Vieira, P. & O'Garra, A. Biology and therapeutic potential of interleukin-10. *J. Exp. Med.* **217**, e20190418 (2020).
43. Wang, I. M., Lin, H., Goldman, S. J. & Kobayashi, M. STAT-1 is activated by IL-4 and IL-13 in multiple cell types. *Mol. Immunol.* **41**, 873–884 (2004).
44. Deimel, L. P., Li, Z., Roy, S. & Ranasinghe, C. STAT3 determines IL-4 signalling outcomes in naive T cells. *Sci. Rep.* **11**, 10495 (2021).
45. Farmer, W. T. & Murai, K. Resolving astrocyte heterogeneity in the CNS. *Front. Cell. Neurosci.* **11**, 1–7 (2017).
46. Tworig, J. M. & Feller, M. B. Müller glia in retinal development: from specification to circuit integration. *Front. Neural Circuits* **15**, 815923 (2022).
47. Jun, J. I. & Lau, L. F. The matricellular protein CCN1 induces fibroblast senescence and restricts fibrosis in cutaneous wound healing. *Nat. Cell Biol.* **12**, 676–685 (2010).
48. Uruski, P. et al. Primary high-grade serous ovarian cancer cells are sensitive to senescence induced by carboplatin and paclitaxel in vitro. *Cell. Mol. Biol. Lett.* **26**, 44 (2021).
49. Wu, X. et al. Opposing roles for calcineurin and ATF3 in squamous skin cancer. *Nature* **465**, 368–372 (2010).
50. Zhu, M. et al. Interleukin-13 promotes cellular senescence through inducing mitochondrial dysfunction in IgG4-related sialadenitis. *Int. J. Oral Sci.* **14**, 29 (2022).
51. Kim, H. D. et al. Interleukin-4 induces senescence in human renal carcinoma cell lines through STAT6 and p38 MAPK. *J. Biol. Chem.* **288**, 28743–28754 (2013).
52. Collado, M. & Serrano, M. Senescence in tumours: evidence from mice and humans. *Nat. Rev. Cancer* **10**, 51–57 (2010).
53. Khattar, E. & Kumar, V. Mitogenic regulation of p27Kip1 gene is mediated by AP-1 transcription factors. *J. Biol. Chem.* **285**, 4554–4561 (2010).
54. Mühl, H. Pro-inflammatory signaling by IL-10 and IL-22: Bad habit stirred up by interferons? *Front. Immunol.* **4**, 18 (2013).
55. Wehinger, J. et al. IL-10 induces DNA binding activity of three STAT proteins (Stat1, Stat3, and Stat5) and their distinct combinatorial assembly in the promoters of selected genes. *FEBS Lett.* **394**, 365–370 (1996).
56. Rex, D. A. B. et al. A comprehensive pathway map of IL-18-mediated signalling. *J. Cell Commun. Signal.* **14**, 257–266 (2020).
57. Zhang, L. M. et al. Interleukin-18 promotes fibroblast senescence in pulmonary fibrosis through down-regulating Klotho expression. *Biomed. Pharmacother.* **113**, 108756 (2019).
58. Kummola, L. et al. IL-4, IL-13 and IFN- γ -induced genes in highly purified human neutrophils. *Cytokine* **164**, 156159 (2023).
59. Yan, W. et al. Cell atlas of the human fovea and peripheral retina. *Sci. Rep.* **10**, 1–17 (2020).
60. Chu, Q. et al. Oxysterol sensing through GPR183 triggers endothelial senescence in hypertension. *Circ. Res.* **135**, 708–721 (2024).
61. Chou, Y.-T. et al. CITED2 functions as a molecular switch of cytokine-induced proliferation and quiescence. *Cell Death Differ.* **19**, 2015–2028 (2012).
62. Troiani, M. et al. Single-cell transcriptomics identifies Mcl-1 as a target for senolytic therapy in cancer. *Nat. Commun.* **13**, 2177 (2022).
63. Sinner, P. et al. Microglial expression of CD83 governs cellular activation and restrains neuroinflammation in experimental autoimmune encephalomyelitis. *Nat. Commun.* **14**, 4601 (2023).
64. Prieto-López, L., Pereiro, X. & Vecino, E. The mechanics of the retina: Müller glia role on retinal extracellular matrix and modelling. *Front. Med.* **11**, 1393057 (2024).
65. Mavrogonatou, E., Papadopoulou, A., Pratsinis, H. & Kletsas, D. Senescence-associated alterations in the extracellular matrix: deciphering their role in the regulation of cellular function. *Am. J. Physiol. Cell Physiol.* **325**, C633–C647 (2023).
66. Matveeva, D. et al. Senescence-associated alterations in matrisome of mesenchymal stem cells. *Int. J. Mol. Sci.* **25**, 5332 (2024).
67. Toba, H. et al. Increased ADAMTS1 mediates SPARC-dependent collagen deposition in the aging myocardium. *Am. J. Physiol. Endocrinol. Metab.* **310**, E1027–E1035 (2016).
68. Kucukdereli, H. et al. Control of excitatory CNS synaptogenesis by astrocyte-secreted proteins hevin and SPARC. *Proc. Natl Acad. Sci. USA* **108**, E440–9 (2011).
69. Wang, S. et al. Inhibition of calcineurin/NFAT signaling blocks oncogenic H-Ras induced autophagy in primary human keratinocytes. *Front. Cell Dev. Biol.* **9**, 720111 (2021).
70. Zhang, M. et al. Fra-1 inhibits cell growth and the Warburg effect in cervical cancer cells via STAT1 regulation of the p53 signaling pathway. *Front. Cell Dev. Biol.* **8**, 579629 (2020).

71. Marsh, S. E. et al. Dissection of artifactual and confounding glial signatures by single-cell sequencing of mouse and human brain. *Nat. Neurosci.* **25**, 306–316 (2022).
72. Tuttle, C. S. L. et al. Cellular senescence and chronological age in various human tissues: a systematic review and meta-analysis. *Aging Cell* **19**, e13083 (2020).
73. Kolkova, K., Novitskaya, V., Pedersen, N., Berezin, V. & Bock, E. Neural cell adhesion molecule-stimulated neurite outgrowth depends on activation of protein kinase C and the Ras-mitogen-activated protein kinase pathway. *J. Neurosci.* **20**, 2238–2246 (2000).
74. Sharma, P. et al. Biphasic role of Tgf- β signaling during Müller glia reprogramming and retinal regeneration in zebrafish. *iScience* **23**, 100817 (2020).
75. Sofroniew, M. V. Astrocyte reactivity: subtypes, states, and functions in CNS innate immunity. *Trends Immunol.* **41**, 758–770 (2020).
76. Lasry, A. & Ben-Neriah, Y. Senescence-associated inflammatory responses: aging and cancer perspectives. *Trends Immunol.* **36**, 217–228 (2015).
77. Vecino, E., Rodriguez, F. D., Ruzafa, N., Pereiro, X. & Sharma, S. C. Glia-neuron interactions in the mammalian retina. *Prog. Retin. Eye Res.* **51**, 1–40 (2016).
78. Bussian, T. J. et al. Clearance of senescent glial cells prevents tau-dependent pathology and cognitive decline. *Nature* **562**, 578–582 (2018).
79. Angelova, D. M. & Brown, D. R. Microglia and the aging brain: are senescent microglia the key to neurodegeneration? *J. Neurochem.* **151**, 676–688 (2019).
80. Rim, C., You, M.-J., Nahm, M. & Kwon, M.-S. Emerging role of senescent microglia in brain aging-related neurodegenerative diseases. *Transl. Neurodegener.* **13**, 10 (2024).
81. Matsudaira, T. et al. Cellular senescence in white matter microglia is induced during ageing in mice and exacerbates the neuroinflammatory phenotype. *Commun. Biol.* **6**, 665 (2023).
82. Flanary, B. E., Sammons, N. W., Nguyen, C., Walker, D. & Streit, W. J. Evidence that aging and amyloid promote microglial cell senescence. *Rejuvenation Res.* **10**, 61–74 (2007).
83. Damani, M. R. et al. Age-related alterations in the dynamic behavior of microglia. *Aging Cell* **10**, 263–276 (2011).
84. Lei, S., Hu, M. & Wei, Z. Single-cell sequencing reveals an important role of SPP1 and microglial activation in age-related macular degeneration. *Front. Cell. Neurosci.* **17**, 1322451 (2023).
85. Bloomfield, C. L. et al. Retinal microglia express more MHC class I and promote greater T-cell-driven inflammation than brain microglia. *Front. Immunol.* **15**, 1399989 (2024).
86. Wolf, J. et al. In-depth molecular profiling specifies human retinal microglia identity. *Front. Immunol.* **13**, 863158 (2022).
87. Torres-Querol, C. et al. Acute ischemic stroke triggers a cellular senescence-associated secretory phenotype. *Sci. Rep.* **11**, 15752 (2021).
88. Matsuda, S. et al. TGF- β in the microenvironment induces a physiologically occurring immune-suppressive senescent state. *Cell Rep.* **42**, 112129 (2023).
89. Dungan, C. M., Wells, J. M. & Murach, K. A. The life and times of cellular senescence in skeletal muscle: friend or foe for homeostasis and adaptation? *Am. J. Physiol. Cell Physiol.* **325**, C324–C331 (2023).
90. Gal, H., Majewska, J. & Krizhanovsky, V. The intricate nature of senescence in development and cell plasticity. *Semin. Cancer Biol.* **87**, 214–219 (2022).
91. Kita, A., Yamamoto, S., Saito, Y. & Chikenji, T. S. Cellular senescence and wound healing in aged and diabetic skin. *Front. Physiol.* **15**, 1344116 (2024).
92. Fan, Y. et al. Senescent-like macrophages mediate angiogenesis for endplate sclerosis via IL-10 secretion in male mice. *Nat. Commun.* **15**, 2939 (2024).
93. Nakamura, R. et al. IL10-driven STAT3 signalling in senescent macrophages promotes pathological eye angiogenesis. *Nat. Commun.* **6**, 7847 (2015).
94. Huang, Y. H. et al. Interleukin-10 induces senescence of activated hepatic stellate cells via STAT3-p53 pathway to attenuate liver fibrosis. *Cell. Signal.* **66**, 109445 (2020).
95. Wan, R. et al. Cellular senescence in asthma: from pathogenesis to therapeutic challenges. *eBioMedicine* **94**, 104717 (2023).
96. Coppé, J. P., Desprez, P. Y., Krtolica, A. & Campisi, J. The senescence-associated secretory phenotype: the dark side of tumor suppression. *Annu. Rev. Pathol. Mech. Dis.* **5**, 99–118 (2010).
97. Min, S. N. et al. Contribution of interleukin-4-induced epithelial cell senescence to glandular fibrosis in IgG4-related sialadenitis. *Arthritis Rheumatol.* **74**, 1070–1082 (2022).
98. Byrns, C. N., Saikumar, J. & Bonini, N. M. Glial AP1 is activated with aging and accelerated by traumatic brain injury. *Nat. Aging* **1**, 585–597 (2021).
99. Leontieva, O. V., Demidenko, Z. N. & Blagosklonny, M. V. MEK drives cyclin D1 hyper-elevation during geroconversion. *Cell Death Differ.* **20**, 1241–1249 (2013).
100. Leontieva, O. V., Lenzo, F., Demidenko, Z. N. & Blagosklonny, M. V. Hyper-mitogenic drive coexists with mitotic incompetence in senescent cells. *Cell Cycle* **11**, 4642–4649 (2012).
101. Bustany, S., Tchakarska, G. & Sola, B. Cyclin D1 regulates p27Kip1 stability in B cells. *Cell. Signal.* **23**, 171–179 (2011).
102. Karakaslar, E. O. et al. Transcriptional activation of Jun and Fos members of the AP-1 complex is a conserved signature of immune aging that contributes to inflammaging. *Aging Cell* **22**, e13792 (2023).
103. Hao, Y. et al. Integrated analysis of multimodal single-cell data. *Cell* **184**, 3573–3587.e29 (2021).
104. Pauly, D. et al. Cell-type-specific complement expression in the healthy and diseased retina. *Cell Rep.* **29**, 2835–2848.e4 (2019).
105. Fadl, B. R. et al. An optimized protocol for retina single-cell RNA sequencing. *Mol. Vis.* **26**, 705–717 (2020).
106. Zappia, L. & Oshlack, A. Clustering trees: a visualization for evaluating clusterings at multiple resolutions. *Gigascience* **7**, giy083 (2018).
107. Peng, Y. R. et al. Molecular classification and comparative taxonomics of foveal and peripheral cells in primate retina. *Cell* **176**, 1222–1237.e22 (2019).
108. Borcherding, N. et al. Mapping the immune environment in clear cell renal carcinoma by single-cell genomics. *Commun. Biol.* **4**, 122 (2021).
109. Tacutu, R. et al. Human ageing genomic resources: new and updated databases. *Nucleic Acids Res.* **46**, D1083–D1090 (2018).
110. Subramanian, A. et al. Gene set enrichment analysis: a knowledge-based approach for interpreting genome-wide expression profiles. *Proc. Natl Acad. Sci. USA* **102**, 15545–15550 (2005).
111. Liberzon, A. et al. Molecular signatures database (MSigDB) 3.0. *Bioinformatics* **27**, 1739–1740 (2011).
112. Benaglia, T., Chauveau, D., Hunter, D. R. & Young, D. S. Mixtools: an R package for analyzing finite mixture models. *J. Stat. Softw.* **32**, 1–29 (2009).
113. Wu, T. et al. clusterProfiler 4.0: a universal enrichment tool for interpreting omics data. *Innovation* **2**, 100141 (2021).
114. Jin, S. et al. Inference and analysis of cell-cell communication using CellChat. *Nat. Commun.* **12**, 1088 (2021).
115. Krämer, A., Green, J., Pollard, J. Jr & Tugendreich, S. Causal analysis approaches in ingenuity pathway analysis. *Bioinformatics* **30**, 523–530 (2014).
116. Yu, C. et al. Microglia at sites of atrophy restrict the progression of retinal degeneration via galectin-3 and Trem2. *J. Exp. Med.* **221**, e20231011 (2024).
117. Li, J. et al. Comprehensive single-cell atlas of the mouse retina. *iScience* **27**, 109916 (2024).

118. Almanzar, N. et al. A single-cell transcriptomic atlas characterizes ageing tissues in the mouse. *Nature* **583**, 590–595 (2020).
119. Li, X. et al. Transcriptional and epigenetic decoding of the microglial aging process. *Nat. Aging* **3**, 1288–1311 (2023).

Acknowledgements

We acknowledge generous funding from the Eolas Foundation. K.B. received a CS-IRG NIG grant (CNIG20nov-0018) from the National Medical Research Council (“NMRC”), Singapore, to support this work. S.S. and G.K. were recipients of the Duke-NUS Medical School (Singapore) PhD Fellowship.

Author contributions

S.S. analysed the scSeq data and was a major contributor in writing the manuscript, data presentation and helped with the lab work for preparing the mouse scSeq dataset, G.K. was a major contributor in writing the manuscript and data presentation, J.F.O. provided major input into the methodology of the analysis of the data, V.C. performed relevant animal procedures, S.A.T. provided major input into preparing the scSeq datasets, E.P. provided major input into the methodology of analysis and interpretation of the scSeq data, J.G.C. had major input into the conceptualisation of the experiments and provided input into the interpretation of the data, writing of the manuscript and data presentation, K.C.B. prepared the scSeq samples and datasets, provided major input into interpreting and analysis of the datasets, major input into conceptualising the study, writing of the manuscript and data presentation. All authors have read, edited, and approved the submitted version of the manuscript.

Competing interests

The authors declare no competing interests.

Ethics approval

All breeding and experimental procedures were undertaken in accordance with the Association for Research for Vision and Ophthalmology Statement for the Use of Animals in Ophthalmic and Research and were approved by the SingHealth Institutional Animal Care and Use Committee (2019/SHS/1534).

Additional information

Supplementary information The online version contains supplementary material available at <https://doi.org/10.1038/s41514-024-00187-9>.

Correspondence and requests for materials should be addressed to Katharina C. Bell.

Reprints and permissions information is available at <http://www.nature.com/reprints>

Publisher’s note Springer Nature remains neutral with regard to jurisdictional claims in published maps and institutional affiliations.

Open Access This article is licensed under a Creative Commons Attribution-NonCommercial-NoDerivatives 4.0 International License, which permits any non-commercial use, sharing, distribution and reproduction in any medium or format, as long as you give appropriate credit to the original author(s) and the source, provide a link to the Creative Commons licence, and indicate if you modified the licensed material. You do not have permission under this licence to share adapted material derived from this article or parts of it. The images or other third party material in this article are included in the article’s Creative Commons licence, unless indicated otherwise in a credit line to the material. If material is not included in the article’s Creative Commons licence and your intended use is not permitted by statutory regulation or exceeds the permitted use, you will need to obtain permission directly from the copyright holder. To view a copy of this licence, visit <http://creativecommons.org/licenses/by-nc-nd/4.0/>.

© The Author(s) 2024